A bioinspired luminescent europium-based probe capable of discrimination between Ag+ and Cu+

Manon Isaac, Sergey A Denisov, Nathan D. Mcclenaghan, Olivier Sénèque

A bioinspired luminescent europium-based probe capable of discrimination between Ag^+ and Cu^+

Manon Isaac,[a] Sergey A. Denisov,[b] Nathan D. McClenaghan,*[b] Olivier Sénèque*[a]

[a] Univ. Grenoble Alpes, CNRS, CEA, IRIG, LCBM (UMR 5249), 38000 Grenoble, France.

[b] Univ. Bordeaux, CNRS, ISM (UMR 5255), 33405 Talence, France.

Email: *olivier.seneque@cea.fr* and *nathan.mcclenaghan@u-bordeaux.fr*

Abstract

Due to their similar coordination properties, discrimination of Cu^+ and Ag^+ by water-soluble luminescent probes is challenging. We have synthesized $LCC4^{Eu}$, an 18 amino acid cyclic peptide bearing a europium complex, that is able to bind one Cu^+ or Ag^+ ion by the side chains of two methionines, a histidine and a 3-(1-naphthyl)-L-alanine. In this system, the naphthyl moiety establishes a cation-π interaction with these cations. It also acts as an antenna for the sensitization of Eu^{3+} luminescence. Interestingly, when excited at 280 nm behaves as a turn-on probe for Ag^+ (+150 % Eu emission) and as a turn-off probe for Cu^+ (–50% Eu^{3+} emission). Shifting the excitation wavelength to 305 nm makes the probe responsive to Ag^+ (+380% Eu^{3+} emission) but not to Cu^+ or other physiological cations. Thus, $LCC4^{Eu}$ is uniquely capable of discriminating Ag^+ from Cu^+. A detailed spectroscopic characterization based on steady state and time-resolved measurements clearly demonstrates that Eu^{3+} sensitization relies on electronic energy transfer from the naphthalene triplet state to the Eu^{3+} excited states and that the cation-π interaction lowers the energy of this triplet state by 700 cm^{-1} and 2400 cm^{-1} for Ag^+ and Cu^+, respectively. Spectroscopic data point to a modulation of the efficiency of the electronic energy transfer caused by the differential red-shift of the naphthalene triplet, deciphering the differential luminescence response of $LCC4^{Eu}$ toward Ag^+ and Cu^+.

Keywords

Peptide – Lanthanide – Silver – Copper – Luminescence

Introduction

Copper is a group 11 element that is an essential micronutrient for living organisms, where it exists in the +I and +II oxidation states.[1,2] It is an important catalytic cofactor for many enzymes involved in electron transfer or oxidative processes. In the oxidizing extracellular environment, copper is in the +II state whereas it is mainly in the +I state in the intracellular environment.[3,4] Since both deficiency and excesses of copper are toxic, its homeostasis is highly regulated in living systems. In order to prevent mobile cellular copper, i.e. copper that is not a cofactor of redox enzymes, from reacting with oxygen and producing reactive oxygen species that are deleterious to the cell, copper(I) is always taken in charge by proteins that bind it tightly and maintain it in the +I state. These proteins generally bind Cu^+ through a set of cysteine, methionine and/or histidine side chains.[5] In particular, the soft S donors of cysteines and methionines favor binding copper in its reduced state.

Silver, which is also a group 11 element, has long been identified as toxic for living organisms. However, being considered as more toxic for bacteria than for humans, it has been used as an antibacterial agent.[6] Conversely to copper, silver exists in biological environments in the +I oxidation state but not the +II one. Cu^+ and Ag^+, with their $[Ar]3d^{10}$ and $[Kr]4d^{10}$ electronic configurations, respectively, share similar coordination properties, especially with respect to protein binding. As a consequence, Ag^+ can replace Cu^+ in proteins.[7–10] This may be detrimental as far as redox proteins are concerned but this can be turned into an advantage when Nature uses very similar proteins in the bacterial CusCFBA or SilCFBA efflux systems to detoxify Cu^+, Ag^+, or both.[11–13]

The toxicity of Ag^+ has elicited the development of molecular Ag^+-responsive fluorescent probes to decipher its impact in biology. Several probes have been described in the literature, but a majority are soluble in organic solvents or water-organic solvent mixtures,[14,15] which limits their use in biological studies. Indeed, only a few probes are soluble in purely aqueous solutions.[16–23] Another issue when developing a Ag^+-responsive probe for biological application is the selectivity with respect to Cu^+. The similarity in coordination properties of these two cations may cause a similar response for both. Interestingly, this issue is rarely considered. While selectivity toward Cu^{2+} is often examined for Ag^+-responsive probes, their behavior towards Cu^+ has only been reported in a few instances for water-soluble probes.[17,24] The propensity of free Cu^+ to disproportionation in aqueous solutions or to oxidation in aerated solutions necessitate strict anaerobic conditions in the presence of a protective reductant such as ascorbate or hydroxylamine[25] and/or a suitable chelating environment (1-3% acetonitrile)[26] to ensure stabilization of Cu in the +I state in water at the micromolar or sub-micromolar concentration range investigated in these studies. Such conditions were not mentioned in these studies, casting doubt on the real Ag^+ / Cu^+ selectivity of these probes. It is also interesting to note that the Cu^+ / Ag^+ selectivity issue is generally not discussed for Cu^+-responsive probes for biological applications, although the selectivity is evaluated for other toxic cations (e.g. Cd^{2+}, Hg^{2+} or Pb^{2+}).[27–30] Therefore, it appears that discrimination between Ag^+ and Cu^+ by responsive fluorescent probes remains a challenge.

We have recently described $LCC1^{Tb}$, a bioinspired Cu^+-responsive Tb^{3+}-based luminescent probe.[31,32] This probe comprises (i) an 18-amino acid cyclic peptide inspired by the copper-binding loop of the protein CusF,[33,34] a metallochaperone involved in Cu^+ trafficking in the periplasm of Gram negative bacteria,[11,12] and (ii) a DOTA[Tb] complex grafted on a lysine side chain of the peptide. $LCC1^{Tb}$ binds one Cu^+ by the side chains of two methionines (Met/M), one histidine (His/H) and a tryptophan (Trp/W). The indole ring of the latter forms a cation-π interaction with Cu^+ as observed in CusF (Figure 1A).[34] Besides being a Cu^+ ligand, the Trp residue serves as an antenna to sensitize Tb^{3+} luminescence: upon excitation of the Trp in its π-π^* transition at ca. 280 nm, Tb^{3+} emission is observed.[35,36] Formation of the $Cu^I{\cdot}LCC1^{Tb}$ complex results in a 6-fold increase of the Tb^{3+} emission. Besides Cu^+, $LCC1^{Tb}$ responds to Ag^+ in a very similar fashion, but it does not respond to any other metal cation.

We have synthesized several Tb^{3+}-based probes derived from $LCC1^{Tb}$ with varied peptide sequences but all of them behaved similarly with respect to Cu^+ and Ag^+.[32] They constitute a perfect example of the difficulty of discriminating between Cu^+ and Ag^+. In this article, we describe a novel probe, $LCC4^{Eu}$, which harnesses Eu^{3+} and a naphthalene antenna instead of Tb^{3+} and tryptophan (Figure 1B). The luminescence of this probe is turned on by Ag^+ but not by Cu^+, providing a clear example of Ag^+ / Cu^+ discrimination in aqueous solution.

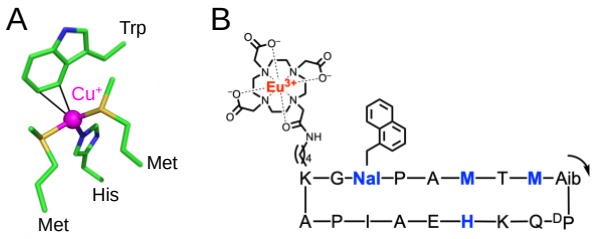

Figure 1. (A) Cu^+ binding site of CusF (pdb 2VB2[34]). (B) Amino acid sequence of $LCC4^{Eu}$, Cu/Ag-chelating amino acids in blue (Nal = 3-(1-naphthyl)-L-alanine; Aib = 2-aminoisobutyric acid; ^{D}P = D-proline). The arrow indicates de N–to–C direction within the cyclic peptide.

Results and discussion

Probe design. $LCC1^{Tb}$ displays a turn-on response to the presence of Cu^+ or Ag^+. A detailed photophysical study of $LCC1^{Tb}$ has shown that the cation-π interaction that is established between Cu^+ or Ag^+ and the indole ring of the tryptophan upon metal binding to the peptide enhances intersystem crossing (ISC) and thus increases the population of the tryptophan excited triplet state, which is the energy transferring state in the Tb^{3+} sensitization process.[31] Therefore, the population of the $Tb(^5D_4)$ excited state increases as well as Tb^{3+} emission, *in fine*. In order to develop probes that emit in the red or the near-infrared using other lanthanides, we decided to focus firstly on Eu-based probes first. Since tryptophan cannot sensitize Eu^{3+} luminescence,[37] naphthalene was chosen as an antenna,[38–40] which features a triplet excited state at ca. 21 300 cm^{-1}.[41] The amino acid sequence of $LCC4^{Eu}$ (Figure 1B) corresponds to the sequence of the parent probe $LCC2^{Tb}$ but with naphthalene and Eu^{3+} replacing tryptophan and Tb^{3+}, respectively.[32] Compared to $LCC1^{Tb}$, this sequence change has almost no consequence on the luminescence properties in response to Cu^+ and Ag^+ but confers higher binding constants (ca. one order of magnitude higher).[32] The synthesis of $LCC4^{Eu}$ is described in the Supporting Information (SI).

Spectroscopic characterization of $LCC4^{Eu}$. $LCC4^{Eu}$ was studied in water buffered with HEPES (10 mM, pH 7.5) except for circular dichroism (CD) measurements for which a phosphate buffer (10 mM, pH 7.0) was used. All solutions were prepared in a glovebox in order to prevent oxidation of Cu^+ by O_2. For comparison purposes, anaerobic conditions were also used for Ag^+-containing samples. For Cu^+-containing samples, NH_2OH (2 mM) was added to the buffer to generate Cu^+ *in situ* by reduction of Cu^{2+} added as a $CuSO_4$ solution. Firstly, titrations of $LCC4^{Eu}$ by Cu^+ and Ag^+ were monitored by CD. The CD spectrum of $LCC4^{Eu}$ (Figure 2A) displays several bands at 198 (–), 216 (–), 228 (+) and 236 nm (–) and is more structured than that of $LCC2^{Tb}$. Upon addition of Cu^+ or Ag^+, a linear evolution of the spectrum is observed up to 1.0 eq. of the metal cation while the spectrum remains unchanged above this value (Figure 2B). This indicates the formation of 1:1 $Cu{\cdot}LCC4^{Eu}$ and $Ag{\cdot}LCC4^{Eu}$ complexes. The CD spectra of the Cu^+ and Ag^+ complexes are very similar. They both display a strong negative signal at 225 nm but with an additional small positive one at 240 nm for Ag^+. These features were already observed with the Cu^+ and Ag^+ complexes of $LCC1^{Tb}$ and $LCC2^{Tb}$.[31,32] Interestingly, a positive CD band appears around 280 nm upon complexation, corresponding to the naphthalene π-π* transition. This may be attributed to restrictions

in the accessible conformations of the 3-(1-naphthyl)alanine side chain that renders the naphthalene moiety CD-active because of a well-defined chiral environment.

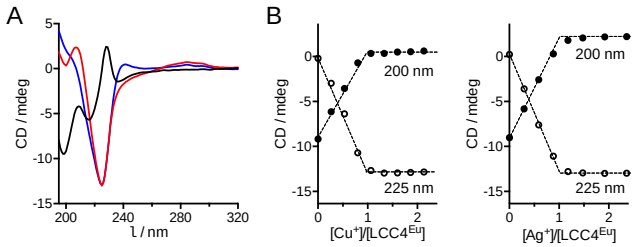

Figure 2. (A) CD spectra of LCC4^{Eu} (black), Cu·LCC4^{Eu} (red) and Ag·LCC4^{Eu} (blue) in phosphate buffer (10 mM, pH 7.0). (B) Evolution of the CD signal at 200 and 225 nm during titrations with Cu^+ (left) and Ag^+ (right).

Complexation of Cu^+ and Ag^+ was then investigated by titrations, monitored by electronic absorption and luminescence spectroscopy, which further confirmed the 1:1 binding stoichiometry (Figure S2 in SI). Upon metal binding, a slight shift (1-2 nm) of the π-π* transition is observed in the absorption spectrum (Figure 3A). A stronger effect is observed for naphthalene fluorescence, with an 80 % and a 70 % quench caused by Cu^+ and Ag^+, respectively (Figure 3B, right). The red-shifted absorption and fluorescence quench are indicative of the formation of the cation-π interaction between Cu^+ or Ag^+ and naphthalene, represented in Figure 3D, as observed for CusF[34] or LCC1^{Tb}.[31] Excitation of the naphthalene at 283 nm results in Eu^{3+} emission with peaks at 580, 595, 616, 654 and 702 nm corresponding to the $^5D_0 \rightarrow {}^7F_J$ (J = 0,1,2,3,4) transitions (Figure 3C, right). The shape of the Eu^{3+} emission spectrum remains unchanged upon Cu^+ and Ag^+ binding as well as the Eu^{3+} emission decay lifetime (τ_{Eu} ≈ 0.63 ms, Table 1). Such a lifetime value is typical of a mono-hydrated (q = 1) Eu^{3+} ion bound to a DOTA-monoamide chelate[42–44] as confirmed by the experimental determination of q for LCC4^{Eu} and Ag·LCC4^{Eu} (Figure S3 and Table S1 in SI). Interestingly, Ag^+ binding induces a 2.5-fold enhancement of intensity of the sensitized Eu^{3+} emission (λ_{ex} = 283 nm) while Cu^+ decreases it by 50 % (Figure 3C, right). The corresponding Eu^{3+} emission quantum yields (Φ_{Eu}^{Nap}) were determined to be 0.018, 0.009 and 0.044 for LCC4^{Eu}, Cu·LCC4^{Eu} and Ag·LCC4^{Eu}, respectively (Table 1). For Cu·LCC4^{Eu} and Ag·LCC4^{Eu} a 2 nm red-shift of the Eu^{3+} luminescence excitation spectrum is observed while naphthalene fluorescence excitation spectra are unshifted. As for LCC1^{Tb}, this can be rationalized by an equilibrium between two forms for the complex: one with the naphthalene bound to Cu^+ or Ag^+ through a cation-π interaction and another one with an unbound naphthalene. The former is non-fluorescent and displays a red-shifted π-π* transition in contrast to the latter (Figure 3B). Therefore, the behavior of LCC4^{Eu} is very similar to the one of LCC1^{Tb} except that Cu^+ decreases the Eu^{3+} emission (×0.5) and Ag^+ increases it (×2.5), while in the case of LCC1^{Tb} both induce an increase in Tb^{3+} emission (×6). Hence, LCC4^{Eu} is able to discriminate between Cu^+ and Ag^+, whereas LCC1^{Tb} is not.

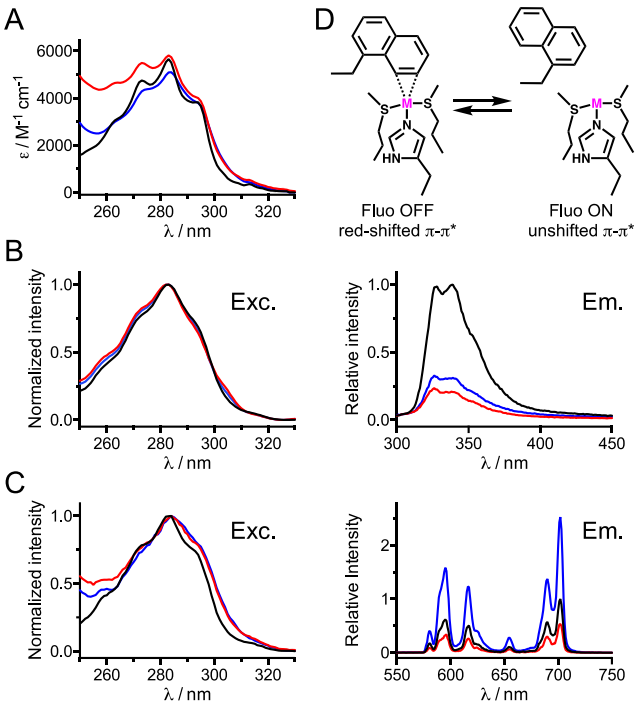

Figure 3. (A) Electronic absorption spectra, (B) fluorescence spectra and (C) time-gated luminescence (delay = 100 µs) spectra of $LCC4^{Eu}$ (black), $Cu{\cdot}LCC4^{Eu}$ (red) and $Ag{\cdot}LCC4^{Eu}$ (blue). In B and C, the emission spectrum is shown on the right (B: λ_{ex} = 290 nm, C: λ_{ex} = 283 nm) and the excitation spectrum is shown on the left (B: λ_{em} = 350 nm, C: λ_{em} = 595 nm, excitation slit = 5 nm). (D) Equilibrium between the two forms of the $M{\cdot}LCC4^{Eu}$ complex (M = Ag or Cu), with or without metal-bound naphthalene. Solutions were prepared in HEPES buffer (10 mM, pH 7.5).

Table 1. Photophysical data for $LCC4^{Ln}$, $Cu{\cdot}LCC4^{Ln}$ and $Ag{\cdot}LCC4^{Ln}$ (Ln = Eu or La). Error on τ^{F}_{Nap}, τ^{P}_{Nap}, τ^{rise}_{Eu} values is estimated at 10 %. Error on τ^{dec}_{Eu} is estimated 0.02 ms. Error on Φ^{Nap}_{Eu} is estimated at 10 %. n.d. = not detected.

Compound	Naphthalene S_1 decay τ^{F}_{Nap} / ns	T_1 decay τ^{P}_{Nap} / µs	Europium $^5D_0$ rise τ^{rise}_{Eu} / µs	$^5D_0$ decay τ^{dec}_{Eu} / ms	τ_R / ms	η_{sens}	Φ^{Eu}_{Eu}	Φ^{Nap}_{Eu}
$LCC4^{Eu}$	2.8 (33%), 17.5 (67%)	n.d.	40	0.63	6.78	0.19	0.093	0.018
$Cu{\cdot}LCC4^{Eu}$	2.5 (38%) 15.2 (62%)	24	25	0.61	6.78	0.10	0.090	0.009
$Ag{\cdot}LCC4^{Eu}$	2.5 (44%) 14.1 (56%)	110	105	0.65	6.78	0.47	0.095	0.044
$LCC4^{La}$	2.3 (8%) 17.9 (92%)	41	–					
$Cu{\cdot}LCC4^{La}$	2.0 (33%) 17.9 (66%)	32	–					
$Ag{\cdot}LCC4^{La}$	2.0 (13%) 17.0 (87%)	53 (10%) 312 (90%)	–					

Mechanistic insight into the Ag^+ / Cu^+ discrimination. The overall quantum yield of sensitized lanthanide luminescence, $\Phi^{antenna}_{Ln}$, is the product of the sensitization efficiency, η_{sens}, and of the intrinsic metal-centered luminescence quantum yield, Φ^{Ln}_{Ln}.[36] In the present case, this translates into Equation 1.

$$\Phi^{Nap}_{Eu} = \eta_{sens} \times \Phi^{Eu}_{Eu} \quad (1)$$

η_{sens} quantifies the efficiency of the population of the Eu^{3+} emissive state ($^5D_0$) starting from photons absorbed by the antenna and Φ_{Eu}^{Eu} quantifies the efficiency of Eu^{3+} emission from its $^5D_0$ excited state. Φ_{Eu}^{Eu} can be determined using Equation 2 from the measured emission lifetime (τ_{Eu}^{dec}) and the radiative lifetime of Eu^{3+} (τ_R) determined from the emission spectrum by Equation 3.[45]

$$\Phi_{Eu}^{Eu} = \tau_{Eu}^{dec}/\tau_R \quad (2)$$

$$\tau_R^{-1} = A_{MD,0}\times n^3\times(I_{tot}/I_{01}) \quad (3)$$

$A_{MD,0}$ is the spontaneous emission probability for the $^5D_0 \rightarrow {}^7F_1$ transition and it is calculated to be 14.65 s^{-1}, n is the refractive index of the medium and I_{tot} and I_{01} are the total area of the corrected Eu^{3+} emission spectrum and the area of the $^5D_0 \rightarrow {}^7F_1$ transition band, respectively. As the Eu^{3+} emission spectrum of $LCC4^{Eu}$ remains unchanged upon Cu^+ or Ag^+ binding, the value of τ_R equals 6.78 ms for the free probe and the Cu^+ and Ag^+ complexes. As τ_{Eu}^{dec} is similar for the three compounds, Φ_{Eu}^{Eu} is almost the same, ca. 0.093 (Table 1). Therefore, the observed differences in Φ_{Eu}^{Nap} are only due to differences in η_{sens} (Table 1). Notably, the sensitization process is ca. 5 times more efficient for $Ag{\cdot}LCC4^{Eu}$ than for $Cu{\cdot}LCC4^{Eu}$ (0.47 vs 0.10).

In order to determine the sensitization pathway, time-resolved emission measurements on the nanosecond and microsecond timescale were performed using streak-camera detection on $LCC4^{Eu}$, $Ag{\cdot}LCC4^{Eu}$ and $Cu{\cdot}LCC4^{Eu}$, as well as their analogues with La^{3+} in place of Eu^{3+}, namely $LCC4^{La}$, $Ag{\cdot}LCC4^{La}$ and $Cu{\cdot}LCC4^{La}$. Unlike Eu^{3+}, La^{3+} is non-luminescent and cannot accept energy from the naphthalene excited states due to empty *f* orbitals. On the nanosecond timescale, for $LCC4^{Eu}$, naphthalene fluorescence is characterized by a bi-exponential decay with a short lifetime of 2.8 ns and a longer one of 17.5 ns. In the case of the Ag^+ and Cu^+ complexes, naphthalene fluorescence, emanating from the species where the naphthalene is not engaged in a cation-π interaction, shows similar lifetimes, as do all three lanthanum analogues. On the microsecond time scale, for $LCC4^{Eu}$, only bands characteristic of Eu^{3+} emission from the $^5D_0$ level are detected, with a rise time of 42 ± 6 µs. On the contrary, for $Ag{\cdot}LCC4^{Eu}$ on this timescale, besides the rise and decay of Eu^{3+} luminescence, an additional broad decaying emission is observed above 480 nm (Figure 4A), which was attributed to naphthalene triplet emission on the basis of its spectrum and decay time in the µs scale (110 ± 15 µs, Table 1). Interestingly, naphthalene triplet emission decay is synchronous with Eu^{3+} luminescence rise (Figure 4B and Table 1). Similar behavior was observed for $Cu{\cdot}LCC4^{Eu}$ (Figure 4B) but with a red-shifted naphthalene phosphorescence (above 500 nm) and shorter (but still synchronous) triplet emission decay and Eu^{3+} luminescence rise (ca. 25 µs, Figure 4D). The broad naphthalene triplet emission could be detected for $Ag{\cdot}LCC4^{La}$ and $Cu{\cdot}LCC4^{La}$ (Figure 4E) but decay times are longer than those of the europium counterparts (Table 1). It was also detected for metal-free $LCC4^{La}$ (Figure 4E, black). The clear correlation between naphthalene triplet emission decay and Eu^{3+} luminescence rise and the shorter characteristic times in the case of the Eu^{3+} compounds compared to La^{3+} indicate that the naphthalene(T_1) is transferring energy to Eu^{3+}. The energy of naphthalene(T_1) was estimated to be 21 500, 20 800 and 19 100 cm^{-1} for $LCC4^{La}$, $Ag{\cdot}LCC4^{La}$ and $Cu{\cdot}LCC4^{La}$, respectively, by taking the wavelength of half-maximum. The value obtained for $LCC4^{La}$ is in good agreement with the one (21 300 cm^{-1}) tabulated for 1-methylnaphthalene.[41] Importantly, both Ag^+ and Cu^+ lower the T_1 state of the antenna engaged in a cation-π interaction by 700 and 2400 cm^{-1}, respectively (Figure 5). These values are similar to those measured in the case of $LCC1^{Tb}$ (600 and 2300 cm^{-1}, respectively).[31]

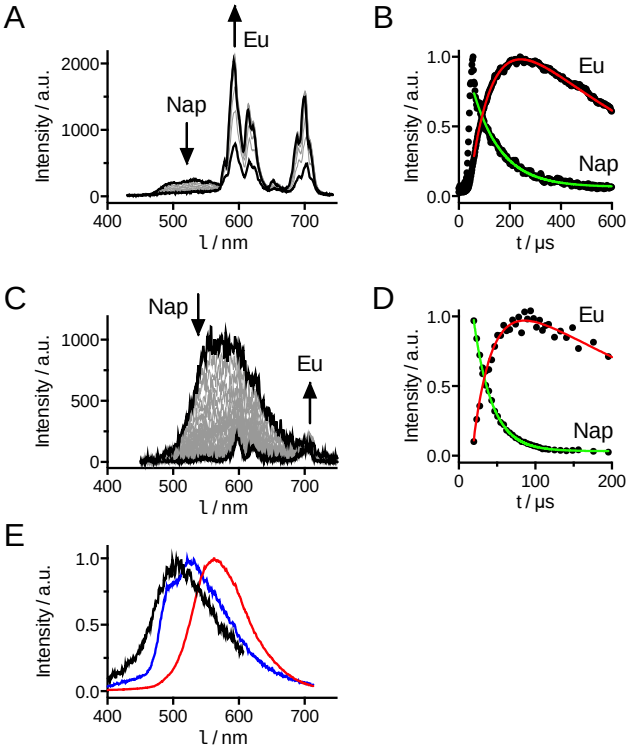

Figure 4. Time-resolved spectroscopy with streak-camera detection (λ_{ex} = 266 nm). (A) Time-resolved emission spectra of Ag·LCC4^{Eu}. (B) Evolution of the naphthalene triplet emission (integrated from 495 to 535 nm) and europium $^5D_0 \rightarrow {}^7F_1$ emission (595 nm). The solid lines correspond to the fit that yielded τ^{P}_{Nap} = 110 µs and τ^{rise}_{Eu} = 105 µs. (C) Time-resolved emission spectra of Cu·LCC4^{Eu}. (D) Evolution of the naphthalene triplet emission (integrated from 500 to 550 nm) and of the deconvoluted europium $^5D_0 \rightarrow {}^7F_4$ emission (680-710 nm). The solid lines correspond to the fit that yielded τ^{P}_{Nap} = 24 µs and τ^{rise}_{Eu} = 25 µs. (E) Naphthalene phosphorescence emission spectra of LCC4^{La} (black), Cu·LCC4^{La} (red) and Ag·LCC4^{La} (blue). Solutions were prepared in HEPES buffer (10 mM, pH 7.5).

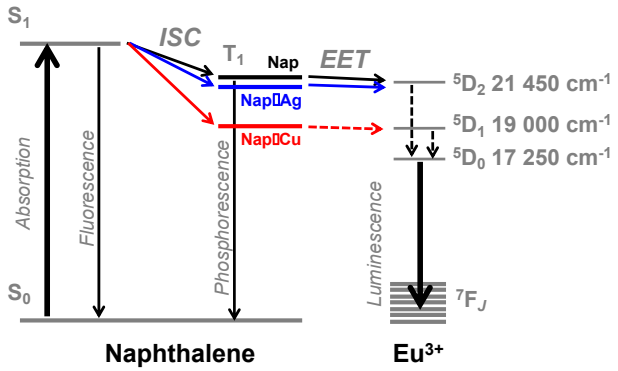

Figure 5. Jablonski-Perrin diagram of LCC4^{Eu} showing pertinent photophysical processes (*ISC* = intersystem crossing, *EET* = electronic energy transfer) and influence of Ag^+ (blue) and Cu^+ (red).

As naphthalene(T_1) is the energy donor state in the sensitization process, the sensitization efficiency η_{sens} can be expressed as the product of the triplet quantum yield Φ_T (also called the intersystem crossing yield) and of the energy transfer efficiency η_{ET} (Equation 3).

$$\eta_{sens} = \Phi_T \times \eta_{ET} \qquad (3)$$

The difference in η_{sens} observed between Cu·LCC4^{Eu} and Ag·LCC4^{Eu} may thus be the result of a difference in intersystem crossing efficiency or energy transfer efficiency or both. Naphthalene derivatives have rather high Φ_T. For instance, for naphthalene and 1-methylnaphthalene the value of Φ_T is 0.75 and 0.58, respectively. A similar value is expected for LCC4^{Eu}. As the cation-π interaction can enhance ISC,[46] Φ_T might be even higher for its Cu^+ and Ag^+ complexes. Considering the values of η_{sens} determined above (Table 1) and assuming Φ_T values varying between 0.6 and 1, the value of η_{ET} falls in the range 0.47–0.78 for Ag·LCC4^{Eu} but drops to 0.10–0.16 for Cu·LCC4^{Eu}. This means that the energy transfer is significantly less efficient for Cu than for Ag. Considering the energy transfer, a collisional / electron exchange (Dexter) mechanism is the most widely-evoked pathway in antenna-to-lanthanide transfer.[36,47–49] A prerequisite for such a pathway would be orbital contact between the naphthalene donor and the europium acceptor, either through preorganization or close approach via dynamic excited state folding. For structural reasons this transfer may be anticipated to be disfavored in the current case. As such, an alternative non-radiative pathway, which we can tentatively consider would be a dipole-dipole (Förster) mechanism. It is often proposed as an alternative mechanism to Dexter one for Ln sensitization. Some examples of Förster resonance energy transfer involving triplet states have been recently reported.[50,51] Equation (4) links η_{ET} to the lifetime of the donor state in the presence (τ_{DA}) and absence (τ_D) of the acceptor in the case of a resonant energy transfer.[52]

$$\eta_{ET} = 1 - \tau_{DA}/\tau_D \quad (4)$$

Values of η_{ET} calculated from τ^P_{Nap} values of Eu (for τ_{DA}) and La (for τ_D) compounds in Table 1 are 0.64 ± 0.10 (considering the 10 % error margin on τ values) and 0.25 ± 0.14 for Ag and Cu, respectively (the averaged lifetime $<\tau^P_{Nap}>$ was used as τ_D for Ag·LCC4^{La}). This in in good agreement with the range of η_{ET} determined above. A good overlap between donor emission and acceptor absorption is required for efficient energy transfer. Eu^{3+} has three possible accepting exited states whose population from the $^7F_0$ ground state match the energy range of naphthalene(T_1) emission (14 000 – 22 000 cm^{-1}): $^5D_0$ (17 250 cm^{-1}), $^5D_1$ (19 000 cm^{-1}) and $^5D_2$ (21 450 cm^{-1}). However, from the selection rules, $^7F_0 \rightarrow {}^5D_0$ transition is formally not allowed ($\Delta J = 0$) and $^7F_0 \rightarrow {}^5D_1$ transition is only Dexter-allowed ($\Delta J = 1$). On the contrary, $^7F_0 \rightarrow {}^5D_2$ transition is Förster-allowed ($\Delta J = 2$). Therefore, naphthalene(T_1) → Eu($^5D_2$) energy transfer appears to be the most favored pathway for LCC4^{Eu} and Ag·LCC4^{Eu}, as naphthalene(T_1) is almost resonant with Eu($^5D_2$). In the case of Cu·LCC4^{Eu}, for which naphthalene(T_1) is 2 300 cm^{-1} below Eu($^5D_2$), energy transfer to Eu($^5D_2$) is unlikely and the accepting state should rather be $^5D_0$ or $^5D_1$. This is possible because selection rules can be relaxed due to thermal population of $^7F_1$ (ca. 30 % at room temperature)[36,53] and *J*–mixing of $^7F_0$ and $^7F_2$. However, a less efficient energy transfer is expected in this case. Therefore, it seems that the differential modulation of the naphthalene(T_1) energy that occurs upon establishment of the cation-π interaction can play a major role in the Ag^+ / Cu^+ discrimination observed with this Eu^{3+}-based probe. Figure 5 summarizes the proposed sensitization pathways.

Practical insight into Ag^+ detection with LCC4^{Eu}. With LCC1^{Tb}, we noticed that the red-shift of the antenna π-π* transition could be used advantageously to magnify the probe response.[31] For instance, while absorption of LCC1^{Tb} and its Cu^+ and Ag^+ complexes are similar at 280 nm, which corresponds to the band maximum, the absorption of LCC1^{Tb} was much lower than that the one of the complexes at 310 nm. Therefore, upon excitation at 310 nm, due to the combination of higher absorption and enhanced ISC, Cu^+ and Ag^+ caused a ca. 55-fold increase of Tb^{3+} emission compared to 6-fold when excitation was at 280 nm.[31] In the case of LCC4^{Eu}, shifting the excitation to 305 nm (5 nm excitation slit) resulted in a 4.8-fold enhancement of Eu^{3+} emission upon Ag^+ binding to LCC4^{Eu} whereas Cu^+ did not induce any change in the intensity of the Eu^{3+} emission (Figure 6A). Hence, under 305 nm excitation, LCC4^{Eu} responds to Ag^+ but not to Cu^+. In order to assess the metal preference

of the probe, we determined its Ag^+ and Cu^+-binding constants, K_{Ag} and K_{Cu}, respectively, by competitive titrations with imidazole as previously described (see SI).[31,42] The binding of Cu^+ proved to be much tighter than Ag^+ ($K_{Cu} = 10^{11.0}$ and $K_{Ag} = 10^{8.1}$). As a consequence, Ag^+ is not able to displace Cu^+ from the Cu·LCC4^{Eu} complex but Cu^+ is able to displace Ag^+. This was confirmed by successive addition of Ag^+ and Cu^+ addition to LCC^{4}Eu (and *vice versa*): under 305 nm excitation, addition of excess Cu^+ to a solution of Ag·LCC4^{Eu} brings the emission level of LCC4^{Eu}, while addition of excess Ag^+ to a solution of Cu·LCC4^{Eu} does not induce any increase of Eu emission. The influence of other physiological cations was also investigated: among Mn^{2+}, Fe^{2+}, Co^{2+}, Ni^{2+}, Zn^{2+}, Na^+, K^+, Ca^{2+} and Mg^{2+}, none of them affected the Ag^+ response (Figure 6B). Therefore, with LCC4^{Eu}, selective detection of Ag^+ is possible in the presence of Cu^+, provided that the concentration of the probe is higher than the total concentration of these two cations. At 10 µM LCC4^{Eu}, a limit of detection (3σ) of 9 nM was determined for Ag^+.

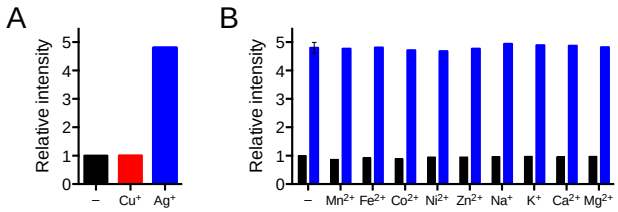

Figure 6. (A) Compared time-gated Eu^{3+} emission (delay = 100 µs) of LCC4^{Eu} (black), Cu·LCC4^{Eu} (red) and Ag·LCC4^{Eu} (blue) under 305 nm excitation. (B) Selectivity diagram showing the integrated time-gated Eu^{3+} emission (λ_{ex} = 305 nm) of LCC4^{Eu} (10 µM) before (black) and after (blue) addition of 1.5 eq. Ag^+ in the presence of various cations (from left to right: none, Mn^{2+}, Fe^{2+}, Co^{2+}, Ni^{2+}, Zn^{2+} (10 µM), Na^+, K^+ (1 mM), Ca^{2+} and Mg^{2+} (1 mM)). Solutions were prepared in HEPES buffer (10 mM, pH 7.5).

Conclusion

LCC4^{Eu}, a novel member of the LCC family of luminescent probes inspired by the copper chaperone CusF, is able to bind Cu^+ and Ag^+ but respond spectroscopically to Ag^+ only when excited at 305 nm. As for other members of the family based on a Tb^{3+} emitter and on a tryptophan antenna, LCC4^{Eu} is able to establish a cation-π interaction between the bound Ag^+/Cu^+ cation and the naphthalene antenna, which modifies the properties of the antenna. In particular, the energy of the triplet excited state is lowered by the cation-π interaction and to a larger extent for Cu^+ than for Ag^+. A detailed time-resolved spectroscopic study has elucidated the sensitization pathway, which involves electronic energy transfer from the naphthalene triplet excited state to europium excited states. It has also revealed a significant difference in the energy transfer efficiency for these two ions. Indeed, we propose that the more efficient energy transfer observed for Ag^+ may arise from a good match between the energy of the donor triplet state and the energy on the europium $^5D_2$ state (allowed process), whereas for Cu^+ electronic energy transfer to $^5D_1$ or $^5D_0$ excited state could occur (non-allowed process). This is to our knowledge, the first time that the ladder-like arrangement of energy levels of lanthanides is used to create a selective responsive luminescent probe.

Acknowledgements

Authors acknowledge the Agence Nationale de la Recherche (ANR-12-BS07-0012), the Labex ARCANE and CBH-EUR-GS (ANR-17-EURE-0003) for financial support.

References

(1) Vest, K. E.; Hashemi, H. F.; Cobine, P. A. The Copper Metallome in Eukaryotic Cells. In *Metallomics and the Cell*; Banci, L., Ed.; Metal Ions in Life Sciences; Springer Netherlands, 2013; pp 451–478. https://doi.org/10.1007/978-94-007-5561-1_13.

(2) Rensing, C.; McDevitt, S. F. The Copper Metallome in Prokaryotic Cells. In *Metallomics and the Cell*; Banci, L., Ed.; Metal Ions in Life Sciences; Springer Netherlands, 2013; pp 417–450. https://doi.org/10.1007/978-94-007-5561-1_12.

(3) Kim, B.-E.; Nevitt, T.; Thiele, D. J. Mechanisms for Copper Acquisition, Distribution and Regulation. *Nat. Chem. Biol.* **2008**, *4* (3), 176–185. https://doi.org/10.1038/nchembio.72.

(4) Lutsenko, S. Copper Trafficking to the Secretory Pathway. *Metallomics* **2016**, *8* (9), 840–852. https://doi.org/10.1039/C6MT00176A.

(5) Davis, A. V.; O'Halloran, T. V. A Place for Thioether Chemistry in Cellular Copper Ion Recognition and Trafficking. *Nat. Chem. Biol.* **2008**, *4* (3), 148–151. https://doi.org/10.1038/nchembio0308-148.

(6) Clement, J. L.; Jarrett, P. S. Antibacterial Silver. *Met. Based Drugs* **1994**, *1* (5–6), 467–482. https://doi.org/10.1155/MBD.1994.467.

(7) Veronesi, G.; Gallon, T.; Deniaud, A.; Boff, B.; Gateau, C.; Lebrun, C.; Vidaud, C.; Rollin-Genetet, F.; Carrière, M.; Kieffer, I.; Mintz, E.; Delangle, P.; Michaud-Soret, I. XAS Investigation of Silver(I) Coordination in Copper(I) Biological Binding Sites. *Inorg. Chem.* **2015**, *54* (24), 11688–11696. https://doi.org/10.1021/acs.inorgchem.5b01658.

(8) Ciriolo, M. R.; Civitareale, P.; Carrì, M. T.; De Martino, A.; Galiazzo, F.; Rotilio, G. Purification and Characterization of Ag,Zn-Superoxide Dismutase from Saccharomyces Cerevisiae Exposed to Silver. *J. Biol. Chem.* **1994**, *269* (41), 25783–25787.

(9) Singh, S. K.; Roberts, S. A.; McDevitt, S. F.; Weichsel, A.; Wildner, G. F.; Grass, G. B.; Rensing, C.; Montfort, W. R. Crystal Structures of Multicopper Oxidase CueO Bound to Copper(I) and Silver(I): Functional Role of a Methionine-Rich Sequence. *J. Biol. Chem.* **2011**, *286* (43), 37849–37857. https://doi.org/10.1074/jbc.M111.293589.

(10) Puchkova, L. V.; Broggini, M.; Polishchuk, E. V.; Ilyechova, E. Y.; Polishchuk, R. S. Silver Ions as a Tool for Understanding Different Aspects of Copper Metabolism. *Nutrients* **2019**, *11* (6), 1364. https://doi.org/10.3390/nu11061364.

(11) Kim, E.-H.; Rensing, C.; McEvoy, M. M. Chaperone-Mediated Copper Handling in the Periplasm. *Nat. Prod. Rep.* **2010**, *27* (5), 711–719. https://doi.org/10.1039/b906681k.

(12) Delmar, J. A.; Su, C.-C.; Yu, E. W. Structural Mechanisms of Heavy-Metal Extrusion by the Cus Efflux System. *Biometals* **2013**, *26* (4), 593–607. https://doi.org/10.1007/s10534-013-9628-0.

(13) Randall, C. P.; Gupta, A.; Jackson, N.; Busse, D.; O'Neill, A. J. Silver Resistance in Gram-Negative Bacteria: A Dissection of Endogenous and Exogenous Mechanisms. *J. Antimicrob. Chemother.* **2015**, *70* (4), 1037–1046. https://doi.org/10.1093/jac/dku523.

(14) Zhang, J. F.; Zhou, Y.; Yoon, J.; Kim, J. S. Recent Progress in Fluorescent and Colorimetric Chemosensors for Detection of Precious Metal Ions (Silver, Gold and Platinum Ions). *Chem. Soc. Rev.* **2011**, *40* (7), 3416–3429. https://doi.org/10.1039/c1cs15028f.

(15) Singha, S.; Kim, D.; Seo, H.; Cho, S. W.; Ahn, K. H. Fluorescence Sensing Systems for Gold and Silver Species. *Chem. Soc. Rev.* **2015**, *44* (13), 4367–4399. https://doi.org/10.1039/C4CS00328D.

(16) Chen, P.; He, C. A General Strategy to Convert the MerR Family Proteins into Highly Sensitive and Selective Fluorescent Biosensors for Metal Ions. *J. Am. Chem. Soc.* **2004**, *126* (3), 728–729. https://doi.org/10.1021/ja0383975.

(17) Iyoshi, S.; Taki, M.; Yamamoto, Y. Rosamine-Based Fluorescent Chemosensor for Selective Detection of Silver(I) in an Aqueous Solution. *Inorg. Chem.* **2008**, *47* (10), 3946–3948. https://doi.org/10.1021/ic800442y.

(18) Neupane, L. N.; Thirupathi, P.; Jang, S.; Jang, M. J.; Kim, J. H.; Lee, K.-H. Highly Selectively Monitoring Heavy and Transition Metal Ions by a Fluorescent Sensor Based on Dipeptide. *Talanta* **2011**, *85* (3), 1566–1574. https://doi.org/10.1016/j.talanta.2011.06.052.

(19) Hu, M.; Fan, J.; Cao, J.; Song, K.; Zhang, H.; Sun, S.; Peng, X. Enhanced Fluorescent Chemosensor for Ag+ in Absolute Aqueous Solution and Living Cells: An Experimental and Theoretical Study. *Analyst* **2012**, *137* (9), 2107–2111. https://doi.org/10.1039/c2an16272e.

(20) Kim, J.-M.; Lohani, C. R.; Neupane, L. N.; Choi, Y.; Lee, K.-H. Highly Sensitive Turn-on Detection of Ag+ in Aqueous Solution and Live Cells with a Symmetric Fluorescent Peptide. *Chem. Commun.* **2012**, *48* (24), 3012–3014. https://doi.org/10.1039/C2CC16953C.

(21) Kleinke, K.; Saran, R.; Liu, J. Label-Free Ag+ Detection by Enhancing DNA Sensitized Tb3+

Luminescence. *Sensors* **2016**, *16* (9), 1370. https://doi.org/10.3390/s16091370.
(22) Panchenko, P. A.; Polyakova, A. S.; Fedorov, Y. V.; Fedorova, O. A. Chemoselective Detection of Ag+ in Purely Aqueous Solution Using Fluorescence "turn-on" Probe Based on Crown-Containing 4-Methoxy-1,8-Naphthalimide. *Mendeleev Commun.* **2019**, *29* (2), 155–157. https://doi.org/10.1016/j.mencom.2019.03.012.
(23) Thamaraiselvi, P.; Duraipandy, N.; Kiran, M. S.; Easwaramoorthi, S. Triarylamine Rhodanine Derivatives as Red Emissive Sensor for Discriminative Detection of Ag+ and Hg2+ Ions in Buffer-Free Aqueous Solutions. *ACS Sustainable Chem. Eng.* **2019**, *7* (11), 9865–9874. https://doi.org/10.1021/acssuschemeng.9b00417.
(24) Hu, Y.; Xiao, Y.; Huang, H.; Yin, D.; Xiao, X.; Tan, W. An Anion-Conjugated Polyelectrolyte Designed for the Selective and Sensitive Detection of Silver(I). *Chem.-Asian J.* **2011**, *6* (6), 1500–1504. https://doi.org/10.1002/asia.201000673.
(25) Xiao, Z.; Gottschlich, L.; van der Meulen, R.; Udagedara, S. R.; Wedd, A. G. Evaluation of Quantitative Probes for Weaker Cu(I) Binding Sites Completes a Set of Four Capable of Detecting Cu(I) Affinities from Nanomolar to Attomolar. *Metallomics* **2013**, *5* (5), 501–513. https://doi.org/10.1039/c3mt00032j.
(26) Kamau, P.; Jordan, R. B. Complex Formation Constants for the Aqueous Copper(I)-Acetonitrile System by a Simple General Method. *Inorg. Chem.* **2001**, *40* (16), 3879–3883. https://doi.org/10.1021/ic001447b.
(27) Hirayama, T.; Van de Bittner, G. C.; Gray, L. W.; Lutsenko, S.; Chang, C. J. Near-Infrared Fluorescent Sensor for in Vivo Copper Imaging in a Murine Wilson Disease Model. *Proc. Natl. Acad. Sci. U. S. A.* **2012**, *109* (7), 2228–2233. https://doi.org/10.1073/pnas.1113729109.
(28) Jia, S.; Ramos-Torres, K. M.; Kolemen, S.; Ackerman, C. M.; Chang, C. J. Tuning the Color Palette of Fluorescent Copper Sensors through Systematic Heteroatom Substitution at Rhodol Cores. *ACS Chem. Biol.* **2018**, *13* (7), 1844–1852. https://doi.org/10.1021/acschembio.7b00748.
(29) Morgan, M. T.; Bagchi, P.; Fahrni, C. J. Designed To Dissolve: Suppression of Colloidal Aggregation of Cu(I)-Selective Fluorescent Probes in Aqueous Buffer and In-Gel Detection of a Metallochaperone. *J. Am. Chem. Soc.* **2011**, *133* (40), 15906–15909. https://doi.org/10.1021/ja207004v.
(30) Morgan, M. T.; Bagchi, P.; Fahrni, C. J. High-Contrast Fluorescence Sensing of Aqueous Cu(I) with Triarylpyrazoline Probes: Dissecting the Roles of Ligand Donor Strength and Excited State Proton Transfer. *Dalton Trans.* **2013**, *42* (9), 3240–3248. https://doi.org/10.1039/c2dt31985c.
(31) Isaac, M.; Denisov, S. A.; Roux, A.; Imbert, D.; Jonusauskas, G.; McClenaghan, N. D.; Sénèque, O. Lanthanide Luminescence Modulation by Cation–π Interaction in a Bioinspired Scaffold: Selective Detection of Copper(I). *Angew. Chem., Int. Ed.* **2015**, *54* (39), 11453–11456. https://doi.org/10.1002/anie.201505733.
(32) Roux, A.; Isaac, M.; Chabert, V.; Denisov, S. A.; McClenaghan, N. D.; Sénèque, O. Influence of Amino Acid Sequence in a Peptidic Cu+-Responsive Luminescent Probe Inspired by the Copper Chaperone CusF. *Org. Biomol. Chem.* **2018**, *16* (31), 5626–5634. https://doi.org/10.1039/C8OB01044G.
(33) Loftin, I. R.; Franke, S.; Roberts, S. A.; Weichsel, A.; Heroux, A.; Montfort, W. R.; Rensing, C.; McEvoy, M. M. A Novel Copper-Binding Fold for the Periplasmic Copper Resistance Protein CusF. *Biochemistry* **2005**, *44* (31), 10533–10540. https://doi.org/10.1021/bi050827b.
(34) Xue, Y.; Davis, A. V.; Balakrishnan, G.; Stasser, J. P.; Staehlin, B. M.; Focia, P.; Spiro, T. G.; Penner-Hahn, J. E.; O'Halloran, T. V. Cu(I) Recognition via Cation-Pi and Methionine Interactions in CusF. *Nat. Chem. Biol.* **2008**, *4* (2), 107–109. https://doi.org/10.1038/nchembio.2007.57.
(35) Weissman, S. I. Intramolecular Energy Transfer: The Fluorescence of Complexes of Europium. *J. Chem. Phys.* **1942**, *10* (4), 214–217. https://doi.org/10.1063/1.1723709.
(36) Bünzli, J.-C. G. On the Design of Highly Luminescent Lanthanide Complexes. *Coord. Chem. Rev.* **2015**, *293*, 19–47. https://doi.org/10.1016/j.ccr.2014.10.013.
(37) Horrocks, W. D.; Bolender, J. P.; Smith, W. D.; Supkowski, R. M. Photosensitized near Infrared Luminescence of Ytterbium(III) in Proteins and Complexes Occurs via an Internal Redox Process. *J. Am. Chem. Soc.* **1997**, *119* (25), 5972–5973.
(38) Quici, S.; Cavazzini, M.; Raffo, M. C.; Botta, M.; Giovenzana, G. B.; Ventura, B.; Accorsi, G.; Barigelletti, F. Luminescence Properties and Solution Dynamics of Lanthanide Complexes Composed by a Macrocycle Hosting Site and Naphthalene or Quinoline Appended Chromophore. *Inorg. Chim. Acta* **2007**, *360* (8), 2549–2557. https://doi.org/10.1016/j.ica.2006.12.040.
(39) Routledge, J. D.; Jones, M. W.; Faulkner, S.; Tropiano, M. Kinetically Stable Lanthanide Complexes Displaying Exceptionally High Quantum Yields upon Long-Wavelength Excitation: Synthesis, Photophysical Properties, and Solution Speciation. *Inorg. Chem.* **2015**, *54* (7), 3337–3345. https://doi.org/10.1021/ic503049m.
(40) Sørensen, T. J.; Kenwright, A. M.; Faulkner, S. Bimetallic Lanthanide Complexes That Display a Ratiometric Response to Oxygen Concentrations. *Chem. Sci.* **2015**, *6* (3), 2054–2059. https://doi.org/10.1039/C4SC03827D.

(41) Montalti, M.; Credi, A.; Prodi, L.; Gandolfi, M. T. Photophysical Properties of Organic Compounds. In *Handbook of Photochemistry, 3rd Ed.*; CRC Press: Boca Raton, 2006.
(42) Isaac, M.; Raibaut, L.; Cepeda, C.; Roux, A.; Boturyn, D.; Eliseeva, S. V.; Petoud, S.; Sénèque, O. Luminescent Zinc Fingers: Zn-Responsive Neodymium Near-Infrared Emission in Water. *Chem.-Eur. J.* **2017**, *23* (46), 10992–10996. https://doi.org/10.1002/chem.201703089.
(43) Cepeda, C.; Raibaut, L.; Fremy, G.; Eliseeva, S. V.; Romieu, A.; Pécaut, J.; Boturyn, D.; Petoud, S.; Sénèque, O. Using Native Chemical Ligation for Site-Specific Synthesis of Hetero-Bis-Lanthanide Peptide Conjugates: Application to Ratiometric Visible or Near-Infrared Detection of Zn2+. *Chem.-Eur. J.* **2020**, *26* (59), 13476–13483. https://doi.org/10.1002/chem.202002708.
(44) Fremy, G.; Raibaut, L.; Cepeda, C.; Sanson, M.; Boujut, M.; Sénèque, O. A Novel DOTA-like Building Block with a Picolinate Arm for the Synthesis of Lanthanide Complex-Peptide Conjugates with Improved Luminescence Properties. *J. Inorg. Biochem.* **2020**, *213*, 111257. https://doi.org/10.1016/j.jinorgbio.2020.111257.
(45) Werts, M. H. V.; Jukes, R. T. F.; Verhoeven, J. W. The Emission Spectrum and the Radiative Lifetime of Eu3+ in Luminescent Lanthanide Complexes. *Phys. Chem. Chem. Phys.* **2002**, *4* (9), 1542–1548. https://doi.org/10.1039/b107770h.
(46) Masuhara, H.; Shioyama, H.; Saito, T.; Hamada, K.; Yasoshima, S.; Mataga, N. Fluorescence Quenching Mechanism of Aromatic-Hydrocarbons by Closed-Shell Heavy-Metal Ions in Aqueous and Organic Solutions. *J. Phys. Chem.* **1984**, *88* (24), 5868–5873. https://doi.org/10.1021/j150668a026.
(47) Parker, D.; Williams, J. A. G. Getting Excited about Lanthanide Complexation Chemistry. *J. Chem. Soc., Dalton Trans.* **1996**, No. 18, 3613–3628. https://doi.org/10.1039/DT9960003613.
(48) Faulkner, S.; Natrajan, L. S.; Perry, W. S.; Sykes, D. Sensitised Luminescence in Lanthanide Containing Arrays and d–f Hybrids. *Dalton Trans.* **2009**, No. 20, 3890–3899. https://doi.org/10.1039/B902006C.
(49) Ward, M. D. Mechanisms of Sensitization of Lanthanide(III)-Based Luminescence in Transition Metal/Lanthanide and Anthracene/Lanthanide Dyads. *Coord. Chem. Rev.* **2010**, *254* (21), 2634–2642. https://doi.org/10.1016/j.ccr.2009.12.001.
(50) Guo, D.; Knight, T. E.; McCusker, J. K. Angular Momentum Conservation in Dipolar Energy Transfer. *Science* **2011**, *334* (6063), 1684–1687. https://doi.org/10.1126/science.1211459.
(51) Cravcenco, A.; Hertzog, M.; Ye, C.; Iqbal, M. N.; Mueller, U.; Eriksson, L.; Börjesson, K. Multiplicity Conversion Based on Intramolecular Triplet-to-Singlet Energy Transfer. *Sci. Adv.* **2019**, *5* (9), eaaw5978. https://doi.org/10.1126/sciadv.aaw5978.
(52) Lakowicz, J. R. *Principles of Fluorescence Spectroscopy*, 3rd ed.; Springer-Verlag: New York, 2006.
(53) Binnemans, K. Interpretation of Europium(III) Spectra. *Coord. Chem. Rev.* **2015**, *295*, 1–45. https://doi.org/10.1016/j.ccr.2015.02.015.